Chemical Engineering Journal 149 (2009) 183–190

Contents lists available at ScienceDirect

Chemical Engineering Journal

journal homepage: www.elsevier.com/locate/cej

Efficiencies of olive kernel gasification combined cycle with solid oxide fuel cells (SOFCs)

C. Athanasiou[a], E. Vakouftsi[b], F.A. Coutelieris[b], G. Marnellos[b], A. Zabaniotou[a,*]

[a] Department of Chemical Engineering, Aristotle University of Thessaloniki, Greece
[b] Department of Management and Engineering of Energy Resources, University of West, Macedonia, Greece

ARTICLE INFO

Article history:
Received 11 June 2007
Received in revised form 9 October 2008
Accepted 17 October 2008

Keywords:
Biomass
Olive kernel
Gasification
SOFC
Conjunction
Electrical efficiency
Thermodynamic analysis

ABSTRACT

The integration of solid oxide fuel cells (SOFCs) in biomass gasification–turbine processes was studied for the estimation of the overall electrical efficiency. Since both processes operate close to 1000 °C, heat integration is one of the benefits of the proposed scheme. Heat generated at the SOFC and the afterburner of the integrated process was found sufficient to cover the demands of gasification and reforming, in any examined case, while a significant heat excess was available to a bottoming thermal cycle for additional power generation. The electrical efficiency of the integrated process was found to overcome 60% of the low heating value of the biomass feed. SOFC's contribution to the overall electrical power output was of the order of 70%, and fuel utilization at the SOFC was recognized as the most crucial operational parameter.

1. Introduction

SOFC cogenerators, due to their high efficiency and relative endurance to microcontaminants, could substantially promote the use of low heating value gaseous fuels (biogas, gasification derived syngas, etc.), in small combined heat and power modules (5–50 kW_{el}) or in larger installations. On the other hand, syngas, from biomass gasification, can disengage SOFCs from hydrogen related obstacles (escalation of production, propagation of distribution infrastructure and safety) and contribute to their commercialization. Furthermore, biomass gasification can upgrade the ecological dimension of SOFC-based power generation, until solar or wind power is able to offer economically attractive large-scale alternatives.

Gasification [1–4] converts biomass, into a gaseous energy carrier of H_2 (5–55%), CH_4 (2–5%), C_2 hydrocarbons (1–3%), CO (5–30%), CO_2 (10–20%), N_2 (0–60% if air is the gasifying agent) and various contaminants (char, ash, tars and oils up to 10 wt.% of the feed), at elevated temperatures, which can be used for power generation in burners, internal combustion engines, turbines and only recently fuel cells [5–7]. Using air, O_2, steam, steam/O_2 mixtures or CO_2 as gasifying agents, gasifiers utilize inert or catalytic particle beds, in a range of reactor configurations, while a number of reviews cover the principles and practices of biomass gasification [1,3]. Hot syngas yields of the process can reach 95–97 wt.% of the biomass feed, while yields of un-condensable gasses can overcome 85%. Syngas composition is determined by the gasifying agent, the temperature, the residence time, the type of biomass, the water content of the raw material and the extent of combustion in the gasifier. Despite the fact that gasification technologies are already available at several MW scale they are still expensive, compared to fossil fuel-based units, and face economical rather than technical barriers for their market intrusion [1,4].

SOFCs have the potential to become a major technology for power generation in the coming decades, due to their high efficiencies (45–60% of the fuel's lower heating value, compared to 30–40% of conventional systems) and extremely low NOx emissions (1/300 compared to coal-based plants). Furthermore, SOFCs are ideal candidates for high quality heat cogeneration, which can be utilized in bottoming thermal engines for additional electric power generation (overall efficiencies, of SOFC–turbine combined cycles can exceed 70%). Currently, up to 250 kW, SOFCs have been proved to operate continuously for more than 5 years, with less than 0.5% voltage degradation. SOFC modules in the range of 1 kW_{el} to 1 MW_{el} are already in demonstrative operation and therefore technologically available to potentially cover a wide range of syngas producing sites. Since 1999 a Siemens–Westinghouse operates a trial 100 kW SOFC, of 46% efficiency, at 950 °C, while Mitsubishi

* Corresponding author. Tel.: +30 2310996274; fax: +30 2310996209.
E-mail address: sonia@cheng.auth.gr (A. Zabaniotou).

1385-8947/$ – see front matter © 2008 Elsevier B.V. All rights reserved.
doi:10.1016/j.cej.2008.10.017

has established a 4 MW system. Smaller modules are already in operation by Chubu Electric Power in Japan, Ceramic Fuel Cells in Australia, Sulzer Hexis in Switzerland, etc. A significant number pilot scale SOFCs has been successfully tested with efficiencies exceeding 45%. Generally, 50 kW to 1 MW SOFCs can be attractive for distributed power generation, in case that investment costs can be reduced even bellow 1000 €/kW from up to 30,000 €/kW today [8–10].

Among various types of fuel cells, SOFCs exhibit advanced fuel flexibility, compared to low-temperature ones, primarily because CO, poison low-temperature electrocatalysts, whereas it contributes as fuel in SOFCs. Although fuel flexibility can promote their commercialization, since pure H_2 is not readily available, performance optimization for a wide variety of $H_2/C_xH_y/CO$ compositions may require significant operating condition, and/or system design changes [11–15]. Nevertheless, a literature survey can reveal a substantial luck of fundamental research concerning gasification-derived-syngas utilization in YSZ-based SOFCs, despite a limited number of studies, most of which refer to digestive biogas and the contiguous landfill gas [16–20].

In this direction, Alderucci et al. [15] carried out a thermodynamic study of a gasifier integrated to a SOFC, as a preliminary approach to assess the electrical efficiency of the overall process. Considering cellulose as the typical biomass feedstock, he predicted overall electrical efficiencies of 47% and 51% for steam and CO_2 gasification, at 700 °C. A Omosun explored the possibility of combining SOFC and biomass gasification, for the generation of power and heat using the gPROMS modelling tool, considering a hot gas cleanup process and a cold gas cleanup process. The electrical and overall efficiency for the hot process were found to be 23 and 60% and for the cold process the efficiencies were 21 and 34%, respectively due to the superior heat management in the first case [18].

Despite the rareness of fundamental studies, and due to the rapidly increased interest for SOFC–biomass conjunction, several pilot efforts of modular, syngas fed, SOFCs are currently under development, for demonstration and investigation purposes [21,22]. Only recently Acumentrics shipped a 5 kW_{el} SOFC to the DOE's National Renewable Energy Lab to investigate the benefits of running a high-efficiency fuel cell system on various biomass-derived fuels along with thermal integration issues. In addition, the inherent ability of SOFCs system to keep the anode and cathode exhaust gases separate is referred to allow the option of SOFC over-fuelling (low utilization) and adding downstream operations for the anode exhaust gases, such as gas or steam turbines [22].

In the present study, the integrated process of the incorporation of solid oxide fuel cells (SOFCs) in the conventional biomass gasification–turbine was studied in terms of thermodynamics for the estimation of the overall electrical efficiency. Experimental data have been obtained for olive kernels gasification – a characteristic agricultural residue of the Mediterranean region – in a fixed bed reactor in the Department of Chemical Engineering of the Aristotle University of Thessaloniki.

2. Flow diagram of the integrated process

Initiating from biomass gasification, technologies based on the use of air as the gasifying agent, are technoeconomically feasible, but produce a low heating value gas (4–8 MJ/m^3) with a 10–25 vol.% H_2 content, depending on H_2 and moisture content of the feedstock, biomass-to-air ratio, temperature, and other parameters. On the other hand, steam-gasification is capable of producing a medium heating value gas (10–16 $MJ/N\,m^3$) gas with 30–60 vol.% H_2 content, but in expense of heat, which in that case should be supplied to the gasifier, in contrast to the exothermic air gasification [1].

In the examined process, and despite the considerable extent of reforming that occurs in the gasifier, due to the presence of moisture in biomass feed, additional steam is supplied in the interceded stage of the syngas reformer. Thus, the biomass–SOFC process of Fig. 1 simulates steam gasification, in terms of H_2 generation, although it does not avoid N_2 dilution of the fuel components. Steam [23] and dry reforming [24,25], primarily of methane, have been extensively investigated. In H_2 rich/C_xH_y lean syngas mixtures, a catalytic reformer can primarily affect H_2/H_2O and CO/CO_2 equilibria, through shift reactions. In this case, according to the gas shift thermodynamics, low temperatures favor H_2 in expense of CO. Both H_2 and CO are SOFC fuels, while H_2 is more favorable. Low temperature gas shift incorporates more H_2 in the process (due to the conversion of steam) and lowers heat requirements (due to the lower temperature and the greater extend of the exothermic reaction), but in expense of CO. On the other hand, high temperatures increase thermal needs of the reformer and decreases H_2, in favor of enhanced kinetics, greater extend of CH_4 reforming, and CO_2's carbon incorporation, due to its conversion to CO.

Fig. 1 depicts the simplified flow diagram of the integrated process, on which the present analyses was based. Along with the gasifier and the SOFC, the process involves a syngas reformer, a burner for the total combustion of both the solid residue from the gasifier and the unburned fuel excess from the cell, and three heat exchangers.

Alkali or chlorine compounds, sulfur compounds and tars, in the produced gas, may damage SOFC as well as the catalyst of an interceded reforming stage. High temperature gas cleaning is reported as the optimum option, for the maximization of the overall efficiency of the gasification–SOFC integrated processes [18]. Tar control can be achieved either during the gasification, by the appropriate primary catalysts, or in reforming stage. Sulphur containing compounds, in biomass derived gases varies from few ppms to few hundreds ppms, depending on feedstock. Nevertheless, sulphur poisons reforming catalysts as well as SOFC anodes, with 1 ppm of sulfur referred as the safety limit of the latest [9]. In the present study, syngas cleaning is considered not to affect the energy balance of the integrated process or the composition of the produced syngas, and will not be taken into account during the thermodynamic calculations.

From the SOFC perspective of the integrated process, power density and fuel utilization determines the overall efficiency of SOFCs, while these parameters are readily affected by the operational cell voltage [9,10]. In the case of the wide range of syngas compositions, the dilution of $H_2/CO/C_xH_y$ combustible agents, results a decrease of the voltage and the cells power density. Even a rush literature survey can reveal a substantial luck of fundamental research concerning syngas utilization in YSZ-based SOFCs, as those incorporated in the proposed project. Rare studies, report power densities reduced to the 1/3 of the corresponding values concerning H_2, due to the dilution of the combustible agents [18–22]. In this context, Sulzer and Hexis have announced efficiencies closed to 27% LHV, of an 1 kW SOFC, operating for 2500 h on bio-derived syngas [21], which is almost 1/2 of the regular SOFC efficiencies on H_2 or reformed natural gas [8–10]. Studies of syngas utilization in intermediate temperature CGO-based SOFCs, also reveal significant current density reductions with H_2 dilution (almost 50% for H_2 dilution from 50 to 10%) [16].

Modelling studies of syngas utilization in SOFCs, predict efficiencies from 23% [18] and 35% [6] to 42% [5] and 50% [26], the latest for theoretical fuel utilizations as high as 80%. Such utilizations are achievable in H_2 or CH_4/H_2O fueled SOFCs, in which open circuit voltages can exceed 1.2 V, allowing operation at overpotentials as high as 0.8 V, with almost optimum power densities [12,18]. This is hardly the case for syngas, where the open circuit voltage might

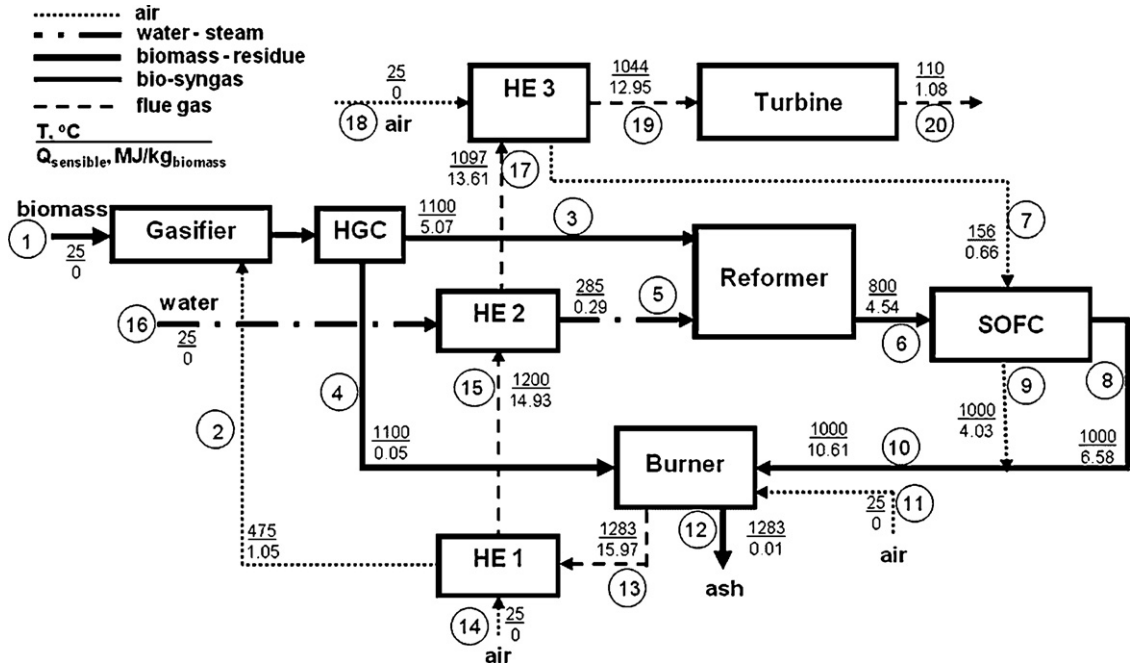

Fig. 1. Simplified flow diagram of the integrated process: (1) biomass inlet, (2) gasification air inlet, (3) produced syngas, (4) gasification residue, (5) steam inlet to reformer, (6) H_2 rich mixture to cell, (7) air inlet to cell, (8) anode's exhaust (unburned fuel), (9) cathode's exhaust (depleted air), (10) gaseous burner feed from the cell, (11) burner's air inlet, (12) ash removal, (13) burner's exhaust to gasifying air heat exchanger, (14) gasification's air inlet to the process, (15) burner exhaust to steam heat exchanger, (16) water's inlet to process, (17) burner's exhaust to SOFC's air heat exchanger, (18) SOFC's air inlet to the process, (19) exhaust gas supply to turbine and (20) process exhaust.

not even reach 0.6 V, and the optimum operational over potential is not grater than 0.4 V [5,6,18,26].

Numerous studies report performance characteristics on steam dilution of H_2, while some of them also examine the effect of fuel composition [27–29]. Furthermore, considering CO, Jiang reported a 60% drop of the current density when CO was diluted to 50% by CO_2 [29]. Generally, H_2 electro-oxidation is two to three times faster than CO's [27,28], due to the insufficient spillover of the latest to the three phase boundary of the electrode–electrolyte interface [30]. This results up to five times lower CO contribution to the cell's power output, compared to H_2, over the most commonly used Ni/YSZ anodes [29,31]. In order to enhance SOFC performance and CO utilization, several composite anodes have been tested [32,33]. Exceptional enhancement of CO contribution to the overall power density, was observed over Cu/CeO_2/YSZ anodes [29,30,34], which was attributed to the expansion of electrochemically active zone of the anode, to the extended surface of O^{2-} conducting CeO_2 [30].

3. Experimental

Experimental data have been obtained for olive kernels gasification in a downdraft fixed bed reactor (height 500 mm and diameter of 12.5 mm) at atmospheric pressure. Gasification took place at a temperature range of 750–950 °C, with air in various equivalence ratios (0.14–0.42), and under atmospheric pressure. In each run the main components of the gas phase were CO, CO_2, H_2 and CH_4. Experimental results showed that gasification with air at high temperatures (950 °C) favored high gas yields and the hydrogen content increased with reactor temperature, while CO, CH_4, light hydrocarbons and tar followed an opposite trend.

Samples of olive kernels (particles with diameters less that 1 mm) were used. The calculation of the air flow rate was determined using a chronometer and a volumetric cylinder, at the start-up of each experimental run. The reactor was placed vertically into the furnace and heating was turned on by setting the controllers at the selected operating temperature. Temperature was measured by a K type thermocouple which was placed vertically inside the reactor and in touch with the biomass sample. Air was used as the gasification medium at varying equivalence ratios; introduced into the reactor through a vertical pipe in a downward flow and was not preheated before entrance (ambient conditions). From each experiment gas was sampled, using an airtight gas sampling bag and analyzed at laboratory's gas chromatograph (Model 6890N, Agilent Technologies). Gas chromatograph (GC) was fitted with two columns HP-PlotQ (30 m × 0.530 mm × 40 μm) and HP-Molsiv (30 m × 0.530 mm × 50 μm), with helium as carrier gas. GC's temperature profile was an isothermal at 50 °C. The standard gas mixture used GC calibration composed from CO, CO_2, H_2, CH_4, C_2H_4 and C_2H_6 1% (v/v) balanced in helium.

Olive kernels produced a maximum gas yield of ~35% (w/w) at equivalence ratio of 0.14 and 950 °C. The maximum heating value of gas from olive kernels was 10.52 MJ/N m^3 at 950 °C and 0.21 equivalence ratio. The production of (CO + H_2) at 950 °C reached the yield of 57% (v/v) of the gas.

4. Assumptions and calculations

The focus of the present study was a parametric analysis of efficiencies and power generation of the integrated biomass gasification–SOFC process. The effect of various parameters such as, extend of biomass gasification, LHV of biomass, steam to carbon excess, turbine electrical efficiency, CO utilization in SOFC has been evaluated. The base for the mass and energy balance calculations was 1 kg of raw biomass per second. Experimental values of olive kernel elemental characteristics are given in Table 1. In the same table, experimental data on gas composition are also presented. Five percent of the massive biomass inlet, correspond to the residue of the gasification process (both char and tar), which was removed in the hot gas cleaning system of Fig. 1. This residue was fed to the burner, where it was

Table 1
Experimental data of olive kernel gasification in the experimental fixed bed reactor.

	Olive kernel
Elemental analysis (%, w/w)	
C	48.61
H	6.41
O	44.98
N	n.a.
S	n.a.
Proximate analysis (%, w/w)	
Moisture	4.59
Volatile mat.	75.56
Fixed carbon	16.39
Ash	3.46
HHV (MJ/kg, dry)	20.39
LHV (MJ/kg, dry)	19.00
Reactor type	Fixed bed
Gasification temperature (°C)	950
Air factor	0.42
Product yields (%, w/w)	
Gas	29.98
Char	30.98
Tar	38.97
Gas composition (%, v/v)	
CO	4.81
CO_2	19.47
H_2	7.78
CH_4	2.99
C_2H_4	0.17
C_2H_6	0.43
LHV gas (MJ/m^3)	2.89

combusted, and its thermal content was considered to be totally recovered.

The heat demand or generation of the gasifier was calculated, by taking into account the experimental lower heating value (LHV) of the olive kernel (19.00 MJ/N m^3 at 950 °C). The specific heat of the olive kernel and char were assumed equal to that of the average wood and wood charcoal (2.3 and 1.01 kJ/kg °C, respectively) [17]. The energy demands of the gasifier, which were assumed adiabatic, were balanced by adjusting its temperature as well as the temperature and the feed rate of the gasifying air supply (Fig. 1). At this point, it must be noted that no heat losses in either the processes or Fig. 1, were taken into account.

According to Fig. 1, the gas at the outlet of the gasifier (at a temperature assumed equal to its operation temperature, 950 °C) entered the reformer, after char and tar residue was separated at the corresponding hot gas cleaning system. Preheated steam was also fed to the reformer, at the appropriate temperature, in order to balance the heat requirements of the endothermic reforming reactions.

In the reformer, the following reactions:

$$CH_4 + H_2O \leftrightarrow CO + 3H_2 \quad (1)$$

$$CO + H_2O \leftrightarrow CO_2 + H_2 \quad (2)$$

$$CH_4 + 2H_2O \leftrightarrow CO_2 + 4H_2 \quad (3)$$

were assumed to be at equilibrium, at the operating temperature, and according to the 250 composition at the inlet. Steam excess, defined as the ratio of its supply to the stoichiometrically required for the total conversion of methane, *was considered as a variable*, in the performed analyses.

H_2, CO, CO_2, CH_4, H_2O and N_2 mixture, from the reformer, was fed in the SOFC anode compartment. CH_4 was assumed not to react with the electrochemical oxygen, while H_2 and CO *utilization were considered as variables*, along with the electrical efficiency of the cell, expressed as the fraction of ΔG, of the reactions taking place, which was directly converted to electricity. The rest of the ΔH of these reactions was regarded as the heat generation at the SOFC. The air inlet to the cell was adjusted so that oxygen concentration at the outlet would be equal to 18 mol%, which is a typical value for SOFCs operation [3,12], while its temperature was controlled by the corresponding heat exchanger, so that the temperature of the cell would be fixed to 950 °C.

Depleted air, from the cathode compartment of the cell, unburned fuel from the anode and tar/char residue from the gasifier, along with an additional ambient air stream, were fed to the burner. The massive flow rate of the latest was adjusted so that the temperature of the burner, and consequently of the outlet, did not exceed 1500 °C.

Total combustion was assumed in the burner, so that its outlet consists only of H_2O, CO_2, O_2 and N_2. The thermal content of this stream was, in all cases, proven sufficient to preheat the air utilized in the gasifier, the reformer's steam supply and the air for the SOFC, at the required temperatures, while a significant amount of heat excess was fed to a steam turbine for the generation of additional power. The *electrical efficiency of the turbine was considered as a variable*, while the un-converted heat supply to the turbine was regarded as the heat generation of the integrated process.

5. Results and discussion

In the analysis that follows, the SOFC temperature was, in every case is equal to 950 °C, the whole process is considered adiabatic, and efficiencies always refer to the LHV of the biomass supply to the integrated process. Electrical efficiencies of the SOFC, the turbine and the overall process are defined as the percentage of the LHV of the biomass fed to the process, which is converted to electricity:

$$\eta_{el}^{SOFC} = \frac{W_{el}^{SOFC}}{LHV}, \quad \eta_{el}^{turbine} = \frac{W_{el}^{turbine}}{LHV}, \quad \eta_{el}^{overal} = \eta_{el}^{SOFC} + \eta_{el}^{turbine}$$

In Fig. 2a, the process and the SOFC's electrical efficiency, as well as the process thermal efficiency, are plotted versus the extent of gasification (inversely expressed as the massive fraction of the un-gasified char/tar residue). As it can be seen, as the un-gasified residue increases (expressed as massive percentage of the biomass feed), η_{el}^{SOFC} and $\eta_{el}^{overall}$ decrease, while $\eta_{thermal}$ increase, as expected, since more fuel is fed directly to the burner, in expense of syngas fed to the SOFC. In Fig. 2b, the electrical power generation of the integrated process is depicted, along with the SOFC's and turbine's contribution to the overall electrical power output. Since less biomass is converted to syngas, SOFC contribution decreases with the increase of gasification char/tar residue. This decrease drifts the overall electrical output, despite the fact that, additional heat generation at the burner enhances the electrical power generation of the turbine. These results are consisted to the assumptions that turbine's efficiency was set equal to 35% of the heat supply, while SOFC's overall efficiency is equal to 51% (85% fuel utilization × 60% efficiency) of the heating value of the syngas supplied. It must be denoted that not all the heat generated by the burner, reach the turbine, because a fraction of this heat is consumed in the heat exchangers of the process. Thus, despite the fact that the same "amount" of combustion occurs throughout the process, regardless the extend of gasification, $\eta_{el}^{overall}$ increases with this extend, since more fuel is supplied to the SOFC.

In Fig. 3, the performance of the integrated process is plotted vs. the LHV of the biomass feed. According to the performed analyses the increase in biomass heat content renders the gasifier more exothermic and increases the heat supply to the turbine. Therefore, the decline of the overall electrical power generation of the pro-

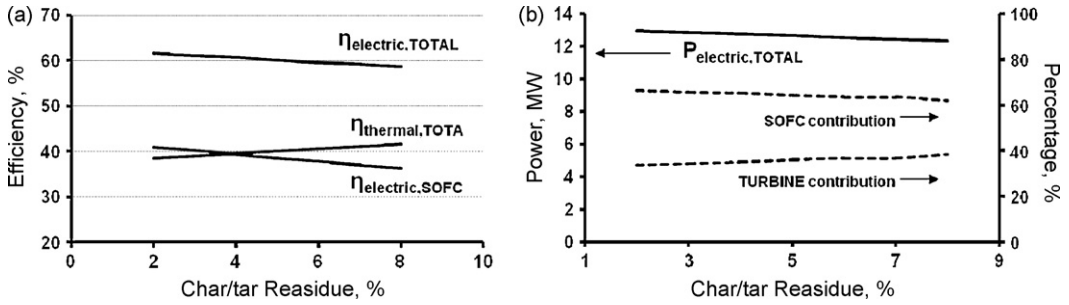

Fig. 2. Dependence of the electrical and thermal efficiency of the integrated process (a), and the contribution of the SOFC and the turbine to the generated electrical power (b), on gasification extend (LHV = 19 MJ/kg, T_{gas} = 950 °C, air equivalent ratio = 0.14 kg/kg, T_{ref} = 800 °C, S/C = 2, T_{cell} = 950 °C, η_{cell} = 60 ΔG%, Uf, H_2 = 85%, Uf, CO = 85%, η_{ST} = 35%).

cess is not proportional to the decline of SOFC's electrical output, due to the fact that more power is generated at the turbine, as the LHV of the biomass increases. This can explain the enhanced contribution of the turbine, depicted in Fig. 3b. Nevertheless, the overall electrical efficiency of the integrated process decreases, despite the increase of the overall electrical output, due to the greater increase of the LHV denominator, during the calculation of the efficiencies depicted in Fig. 3.

According to Fig. 4b, the increase of steam excess at the reformer of the integrated process results a small initial increase of the overall electrical power output, followed by a constant decrease. The same behavior is also noticed in Fig. 4a, concerning the overall efficiency. The maximum electrical output and efficiency corresponds to steam supply to the reformer equal to two times the stoichiometrically required steam, for the total conversion of methane. Nevertheless the efficiency of the SOFC, as well as its contribution to the electrical power generation, increases constantly with steam excess. Here, it must be noted that steam excess influences the overall process in two manners. On one hand it shifts the equilibrium of reaction (3) to the products, which results additional hydrogen incorporation and enhanced power generation in the SOFC. On the other hand it increases the heat demands of the reformer and decreases the thermal input to the turbine, as well as the thermal output of the process. Accordingly, overall power generation and efficiency increase as long as that additional hydrogen incorporation to the process overcomes the additional heat requirements of the reformer, while this situation is readily affected by the relative efficiencies of the turbine and the SOFC.

The situation is quite similar in case of Fig. 5, where the performance parameters of the integrated process are plotted vs. the temperature of the reformer. The increase of this temperature shifts the equilibrium of the reactions in the reformer to the products, but requires additional heat supply to the reformer. The situation becomes more complicated due to the fact that in order to adjust the temperature of the adiabatic reformer to the appropriate value, steam excess should be altered. The overall result is a constant increase of the SOFC efficiency, which is accompanied by a proportional increase in the overall efficiency and power output, until almost 850 °C. Above this temperature, SOFC efficiency tends to a limiting value, and the overall efficiency decrease, since the increase of hydrogen generation in the reformer cannot counterbalance heat consumption. Above 900 °C, the overall power generation decreases significantly, due to a rapid deterioration of turbines contribution and despite the sharp increase of the SOFC's contribution.

Demonstrative SOFC stacks are referred to achieve electrical efficiencies of the order of 60% of the free energy of the electro-oxidation reaction reactions occurring at the anode [8,9]. Thus, Fig. 6 presents the dependence of the performance of the integrated process on the electrical efficiency of the incorporated SOFC. As expected, the increase of the SOFC efficiency increases the overall electrical power output, in expense of the thermal generation of the process.

Nevertheless, the SOFC electrical efficiency, the total thermal efficiency and the total electrical efficiency can reach the values of 42, 38 and 62%, respectively. Another parameter that significantly affects the SOFC contribution to the overall efficiency of the integrated process of Fig. 1, is the fuel utilization. As mentioned above, fuel utilization depends on the open circuit and the operational voltage of the cell. Concerning hydrogen, an operating voltage of 300–500 mV, per unit cell, is readily achievable when hydrogen content at the anode exhaust is almost 15%. This means that, introducing a syngas mixture of 20% hydrogen, to the SOFC, the usual operating voltage obtains about 25% fuel utilization [5,6,16,18–21,26]. By taking into account that hydrogen fuelled SOFCs can achieve fuel utilization of the order of 85%, Fig. 7 depicts the effect of fuel utilization, on the SOFC's efficiency and the overall efficiency of the integrated process.

From Fig. 7a, it can be seen that by increasing fuel utilization from 15 to 85%, the over efficiency increases from 40 to about 60%. This result denotes the importance of fuel utilization, for the effectiveness of the integrated process. Syngas's fuel components are primarily H_2 and CO. Despite the fact that the free energy of

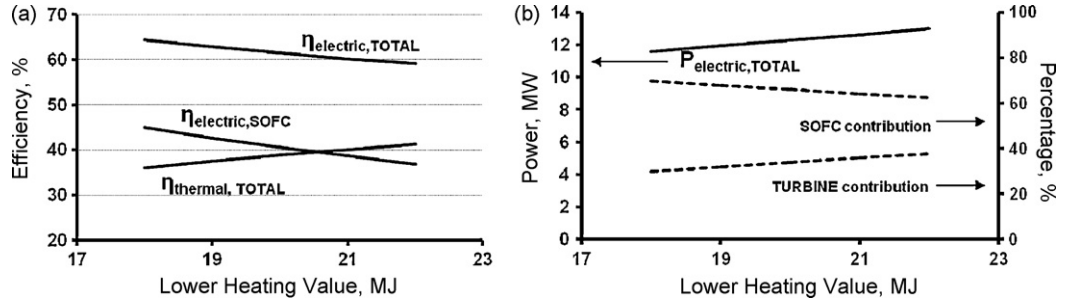

Fig. 3. Dependence of the electrical and thermal efficiency of the integrated process (a), and the contribution of the SOFC and the turbine to the generated electrical power (b), on biomass lower heating value (T_{gas} = 950 °C, Air equivalent ratio = 0.14, T_{ref} = 800 °C, S/C = 2, T_{cell} = 950 °C, η_{cell} = 60 ΔG%, Uf, H_2 = 85%, Uf, CO = 85%, η_{ST} = 35%).

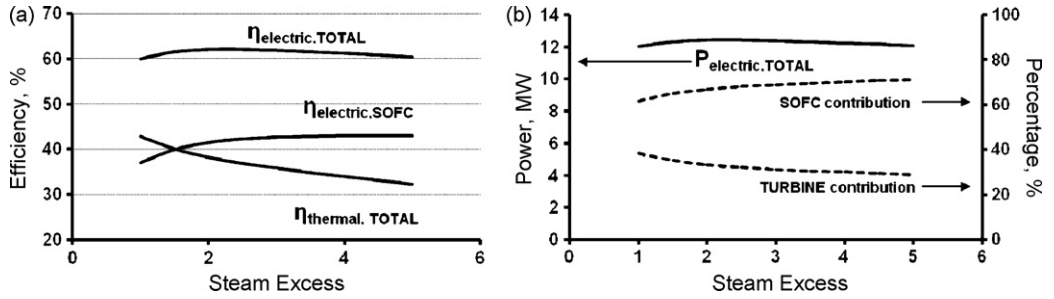

Fig. 4. Dependence of the electrical and thermal efficiency of the integrated process (a), and the contribution of the SOFC and the turbine to the generated electrical power (b), on steam to carbon excess (LHV = 19 MJ/kg, T_{gas} = 950 °C, air equivalent ratio = 0.14, T_{ref} = 800 °C, T_{cell} = 950 °C, η_{cell} = 60 ΔG%, Uf, H_2 = 85%, Uf, CO = 85%, η_{ST} = 35%).

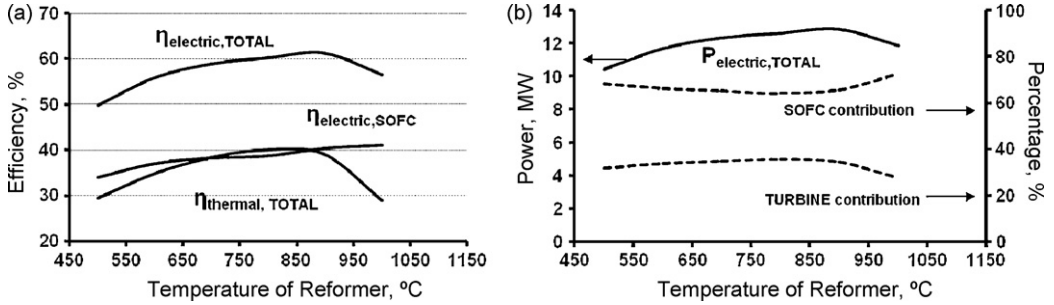

Fig. 5. Dependence of the electrical and thermal efficiency of the integrated process (a), and the contribution of the SOFC and the turbine to the generated electrical power (b), on reformer's temperature (LHV = 19 MJ/kg, T_{gas} = 950 °C, air equivalent ratio = 0.14, S/C = 2, T_{cell} = 950 °C, η_{cell} = 60 ΔG%, Uf, H_2 = 85%, Uf, CO = 85%, η_{ST} = 35%).

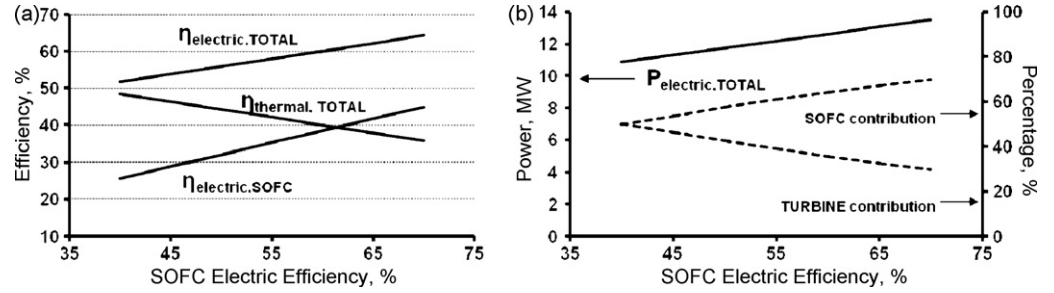

Fig. 6. Dependence of the electrical and thermal efficiency of the integrated process (a), and the contribution of the SOFC and the turbine to the generated electrical power (b), on SOFC efficiency (LHV = 19 MJ/kg, T_{gas} = 950 °C, Air equivalent ratio = 0.14, T_{ref} = 800 °C, S/C = 2, T_{cell} = 950 °C, Uf, H_2 = 85%, Uf, CO = 85%, η_{ST} = 35%).

CO's combustion (283 kJ/mol) is higher than that of hydrogen's (242 kJ/mol), and the kinetics of its oxidation faster, H_2 is considered as a more effective fuel for SOFCs, due to the special characteristics of anodic reactions. In SOFC anodes, electro-oxidation primarily occurs at the three phase boundary between the gas phase, the electrode and the electrolyte. Therefore, adsorbed fuel species on the electrodes surface have to diffuse to the three phase boundary. This process is quite fast for the small hydrogen atoms, whether it is rather slow for the adsorbed CO molecules [27,28,30]. Despite the fact that several anode composites, that facilitates CO electro-oxidation, have been developed in the laboratory [32,33], it is not ensured that in larger scale SOFC applications, CO utilization will be the same with that of hydrogen, as assumed in Fig. 7. Thus, in Fig. 8 depict the effect of CO utilization, on the SOFC and the inte-

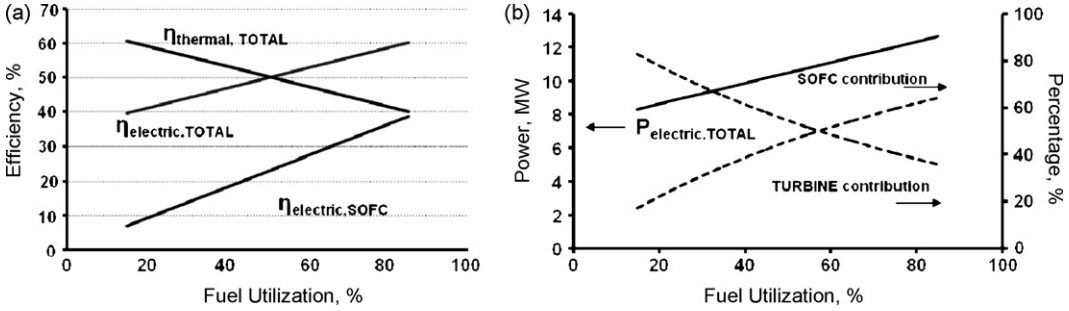

Fig. 7. Dependence of the electrical and thermal efficiency of the integrated process (a), and the contribution of the SOFC and the turbine to the generated electrical power (b), on fuel (CO and H_2) utilization in the SOFC (LHV = 19 MJ/kg, T_{gas} = 950 °C, air equivalent ratio = 0.14, T_{ref} = 800 °C, S/C = 2, T_{cell} = 950 °C, η_{cell} = 60 ΔG%, η_{ST} = 35%).

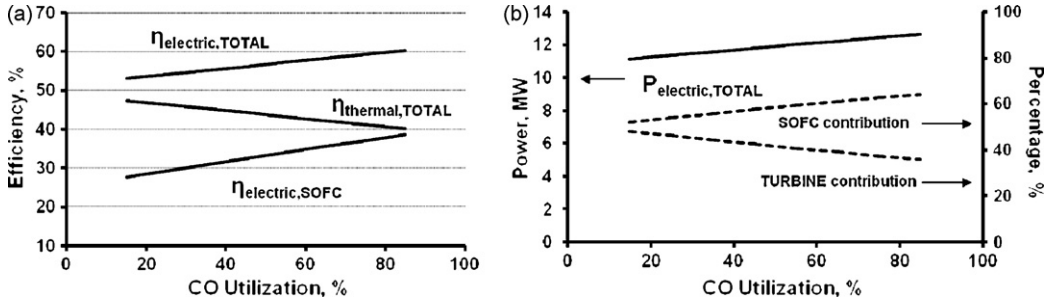

Fig. 8. Dependence of the electrical and thermal efficiency of the integrated process (a), and the contribution of the SOFC and the turbine to the generated electrical power (b), on CO utilization in the SOFC (LHV = 19 MJ/kg, T_{gas} = 950 °C, air equivalent ratio = 0.14 T_{ref} = 800 °C, S/C = 2, T_{cell} = 950 °C, η_{cell} = 60 ΔG%, Uf, H_2 = 85%, η_{ST} = 35%).

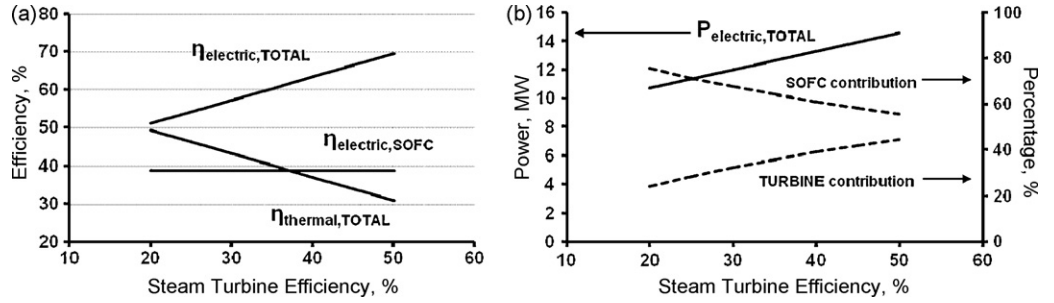

Fig. 9. Dependence of the electrical and thermal efficiency of the integrated process (a), and the contribution of the SOFC and the turbine to the generated electrical power (b), on turbine efficiency (LHV = 19 MJ/kg, T_{gas} = 950 °C, air equivalent ratio = 0.14, T_{ref} = 800 °C, S/C = 2, T_{cell} = 950 °C, η_{cell} = 60 ΔG%, Uf, H_2 = 85%, Uf, CO = 85%).

grated process performance. From Figure 8a, it can be seen that, for 85% H_2 utilization, the increase of CO conversion from 15 to 85%, results an increase of overall efficiency from 52 to 60%. This increase by almost 15% denotes the significance of CO utilization for the integrated process.

Finally, Fig. 9 presents the effect of the turbine's efficiency on the overall performance of the integrated process. As it is obvious from Fig. 9a, the SOFC can achieve an overall 40% conversion of biomass heating value to electricity. The incorporation of a bottoming turbine, in order to utilize the SOFC exhaust heat and un-burned fuel along with the thermal content of the gasification residue, results a substantial increase of the overall efficiency by almost 25% (from less than 40 to more than 50%), when the intrinsic electrical efficiency of the turbine is only 20%. This enhancement can overcome 60% (from less than 40 to almost 70%), in case that the turbine's efficiency can reach 50%. Nevertheless, even in the last case, turbines contribution to the overall power generation falls short the contribution of the SOFC, as it can be seen from Fig. 9b.

6. Conclusions

The aim of the present analysis is to examine the effectiveness of incorporating an SOFC in the conventional gasification–turbine process. This incorporation would be justified if the SOFC is able to substantially upgrade the efficiency of the biomass-to-energy conversion. As it can be resulted from the present analysis, which, nevertheless, deals with the ideal case of thermodynamic efficiencies under no thermal losses operation, SOFC contribution to the overall power generation usually exceeds 60% while integrated gasification in combined cycles with, e.g. engines, turbines, etc., gives overall efficiencies (45–50%) [31]. Furthermore, the overall electrical efficiency of the integrated process for olive kernel can, ideally, reach 62% of the heating value of the biomass feed, whereas conventional technologies, like turbines, can only randomly reach 40% of the heat supplied to their inlet. Even in the case of 15% fuel utilization (Fig. 7), SOFC can contribute more than 20% of the overall power output.

Acknowledgments

The project was funded by the Ministry of Education of Greece and EC under the program PYTHAGORAS II.

References

[1] A.V. Bridgwater, Renewable fuels and chemicals by thermal processing of biomass, Chemical Engineering Journal 91 (2003) 87–102.
[2] J. Gil, J. Corella, M. Aznar, M. Caballero, Biomass gasification in atmospheric and bubbling fluidized bed: effect of the type of gasifying agent on the product distribution, Biomass and Bioenergy 17 (5) (1999) 389–403.
[3] D. Sutton, B. Kelleher, J.R.H. Ross, Review of literature on catalysts for biomass gasification, Fuel Processing Technology 73 (2001) 155–173.
[4] K. Maniatis, Progress in biomass gasification: an overview, in: A.V. Bridgwater (Ed.), Progress in Thermochemical Biomass Conversion, Blackwell Scientific Publications, Oxford, UK, 2001, pp. 1–32.
[5] J. Van Herle, Y. Membrez, O. Bucheli, Biogas as a fuel source for SOFC cogenerators, Journal of Power Sources 127 (2004) 300–312.
[6] J. Van Herle, F. Marechal, S. Leuenberger, D. Favrat, Energy balance model of a SOFC cogenerator operated with biogas, Journal of Power Sources 118 (2003) 375–383.
[7] N. Lymberopoulos, Fuel cells and their application in bio-energy, Project Technical Assistant Framework Contract (EESD Contract No. NNE5-PTA-2002-003/1), February 2005.
[8] O. Yamamoto, Solid oxide fuel cells: fundamental aspects and prospects, Electrochimica Acta 45 (2000) 2423–2435.
[9] S. Singhal, Advances in solid oxidefuel cell technology, Solid State Ionics 135 (2000) 305–313.
[10] G. Marnellos, C. Athanasiou, S. Makridis, E. Kikkinides, Integration of hydrogen energy technologies in autonomous power systems, in: Zoulias, I. Emmanuel (Eds.), Hydrogen-based Autonomous Power Systems, Springer, London, 2008, ISBN 978-1-84800-246-3.
[11] H. Kim, S. Park, J. Vohs, R. Gorte, Direct oxidation of liquid fuels in a solid oxide fuel cell, Journal of the Electrochemical Society 148 (7) (2001) A693–A695.
[12] R. Sidwell, W. Grover Coors, Large limits of electrical efficiency in hydrocarbon fuelled SOFCs, Journal of Power Sources 143 (2005) 166–172.
[13] Y. Yi, A. Rao, J. Brouwer, G. Samuelsen, Fuel flexibility study of an integrated 25 kW SOFC reformer system, Journal of Power Sources 144 (2005) 67–76.
[14] K. Eguchi, H. Kojo, T. Takeguchi, R. Kikuchi, K. Sasaki, Fuel flexibility in power generation by solid oxide fuel cells, Solid State Ionics 152/153 (2002) 411–416.

[15] A. Alderucci, P. Antonucci, G. Maggio, N. Giordano, V. Antonucci, Thermodynamic analysis of SOFC fuelled by biomass-derived gas, International Journal of Hydrogen Energy 19 (4) (1994) 369–376.
[16] S. Baron, N. Branton, A. Atkinson, B. Steele, R. Rudkin, The impact of wood derived gasification gases on Ni–CGO anodes in intermediate temperatures SOFCs, Journal of Power Sources 126 (2004) 58–66.
[17] C. Athanasiou, F. Coutelieris, E. Vakouftsi, V. Skoulou, E. Antonakou, G. Marnellos, A. Zabaniotou, From biomass to electricity through integrated gasification/SOFC system-optimization and energy balance, International Journal of Hydrogen Energy 32 (3) (2007) 337–342.
[18] A.O. Omosun, A. Bauen, N.P. Brandon, C.S. Adjiman, D. Hart, Modelling system efficiencies and costs of two biomass-fuelled SOFC systems, Journal of Power Sources 131 (2004) 96–106.
[19] J. Staniforth, K. Kendall, Syngas powering a small tubular SOFC, Journal of Power Sources 71 (1998) 275.
[20] J. Staniforth, K. Kendall, Cannock landfill gas powering a small tubular SOFC—a case study, Journal of Power Sources 86 (2000) 401.
[21] M. Jenne, T. Zahringer, A. Schuler, D. Moos Hart, Sulzer HEXIS SOFC systems for syngas and heating oil, in: U. Bossel (Ed.), Proceedings of the 5th European Solid Oxide Fuel Cell Forum, Lucerne, Switzerland, European Forum Secretariat, Oberrohrdorf, Switzerland, July 2002, pp. 460–466.
[22] Acumentrics ships SOFC for NREL syngas study, Fuel Cell Bulletin (January) (2005).
[23] J.N. Armor, The multiple roles for catalysis in the production of H_2, Applied Catalysis A-General 176 (1999) 159–176.
[24] X. Verykios, Catalytic dry reforming of natural gas for the production of chemicals and hydrogen, International Journal of Hydrogen Energy 28 (2003) 1045–1063.
[25] X. Verykios, Mechanistic aspects of the reaction of CO_2 reforming of methane over Rh/Al_2O_3 catalyst, Applied Catalysis A: General 255 (2003) 101–111.
[26] J. Van Herle, F. Marechal, S. Leuenderger, Y. Membrez, O. Bucheli, D. Favrat, Process flow model of SOFC system supplied with sewage syngas, Journal of Power Sources 131 (2004) 127–141.
[27] M. Brown, S. Primdahl, M. Moggensen, Structure/performance relations for Ni/yttria-stabilized zirconia anodes for solid oxide fuel cells, Journal of Electrochemical Society 147 (2000) 475–485.
[28] Y. Matsuzaki, I. Yasuda, Electrochemical oxidation of H_2 and CO in a H_2–H_2O–CO–CO_2 system at the interface of a Ni–YSZ cermet electrode and YSZ electrolyte, Journal of Electrochemical Society 147 (2000) 1630–1635.
[29] Y. Jiang, A. Virkar, Fuel composition, diluent effect on gas transport and performance of anode-supported SOFCs, Journal of Electochemical Society 150 (2003) A942–A951.
[30] C. Lu, W. Worrell, J. Vohs, R. Gorte, A comparison of Cu–ceria–SDC and Au–ceria–SDC composites for SOFC anodes, Journal of Electrochemical Society 150 (2003) A1357–A1359.
[31] O. Costa-Nunes, R. Gorte, J. Vohs, Comparison of the performance of Cu–CeO_2–YSZ and Ni–YSZ composite SOFC anodes with H_2, CO and syngas, Journal of Power Sources 141 (2005) 241–249.
[32] R. Gorte, J. Vohs, S. McIntosch, Recent developments on anodes for direct fuel utilization in SOFC, Solid State Ionics 175 (2004) 1–6.
[33] J. Vohs, S. Park, R. Gorte, Direct oxidation of hydrocarbons in a solid-oxide fuel cell, Nature 404 (2000) 265–267.
[34] S. Lee, J. Vohs, R. Gorte, A study of SOFC anodes based on Cu–Ni and Cu–Co bimetallics in CeO_2–YSZ, Journal of Electrochemical Society 151 (2004) A1319–1323.